Chapter 2
Investigation on the identification of Spatially-Varying Elastic and Damping Properties in Beams and Plates Using Physics-Informed Neural Networks

Morvan Ouisse, Maxime Auger, João Gabriel Oliveira Aveiro, Roberta Tittarelli, Valentin Calisti, Rafael Teloli, Emmanuel Ramasso, Patrice Le Moal

Abstract This work presents a Physics-Informed Neural Network (PINN) approach for the identification of spatially-varying elastic and damping properties in structures subjected to bending. The study focuses on beams and plates made of non-homogeneous materials, where conventional identification techniques often struggle to accurately resolve local variations in mechanical properties due to limited data or the need for strong prior assumptions.

The proposed method investigates the ability of PINNs to embed the governing partial differential equations of structural dynamics directly into the training process of neural networks. By incorporating the equations of motion for bending, including both stiffness and damping contributions, into the loss function, the network learns not only to fit the observed displacement data, but also to satisfy the underlying physics. This allows the identification of spatial distributions of the Young's modulus and damping coefficients without requiring explicit meshing or parameter regularization.

The approach is validated on simulated and experimental test cases involving non-uniform beams and plates, for steady-state flexural responses. Results discuss the ability of the PINN framework of accurately reconstructing complex spatial profiles of material properties, even with sparse and noisy measurements. The method is checked in terms of robustness and generalizability, to investigate its capability to become a promising tool for non-destructive testing and material characterization in advanced mechanical systems.

Keywords PINN · identification · damping

Introduction

Decision-making in engineering requires models that balance performance, validity and cost-effectiveness. Physics-based simulations, often formulated with partial differential equations (PDEs), serve as virtual prototyping tools to analyze complex structures. When analytical solutions are unavailable, numerical methods such as finite elements (FE) are employed, though they face challenges related to boundary conditions, meshing, and computational cost.

In parallel, data-driven methods have emerged, exploiting machine learning to address tasks from regression to structural monitoring. Despite their flexibility and universal approximation capabilities, such models often suffer from lack of interpretability, instability, and poor extrapolation [1, 2]. This motivates approaches that combine data with physical principles.

Physics-informed machine learning addresses this need by embedding physical laws into the training process [3]. Among these, Physics-informed neural networks (PINNs) [4] have gained traction, with applications in continuum mechanics [5], thermochemical processes [6], and fluid dynamics [7]. PINNs incorporate PDEs and conservation laws directly into the loss

Morvan Ouisse · Maxime Auger · João Gabriel Oliveira Aveiro · Roberta Tittarelli · Valentin Calisti · Rafael Teloli · Emmanuel Ramasso · Patrice Le Moal
Université Marie et Louis Pasteur, SUPMICROTECH, CNRS
Institut FEMTO-ST
F-25 000 Besançon, France
e-mail: morvan.ouisse@femto-st.fr; maxime.auger@femto-st.fr; joao.oliveira_aveiro@ens2m.org; roberta.tittarelli@femto-st.fr; valentin.calisti@femto-st.fr; rafael.teloli@femto-st.fr; emmanuel.ramasso@femto-st.fr; patrice.lemoal@femto-st.fr

B. J. Dilworth et al. (eds.), *Topics in Modal Analysis & Parameter Identification, Vol. 9*, Conference Proceedings of the Society for Experimental Mechanics Series, https://doi.org/10.1007/978-3-031-68180-6_2

function, bridging the gap between data and physics. Recent works have applied them to solid mechanics [8], viscoelasticity [9], and dynamical systems [10, 11].

However, their use in inverse problems for structural dynamics remains limited, particularly where damping and frequency-domain analysis are central [12, 13]. Existing studies on beam-like structures [14, 15, 16] do not validate with experimental data and often overlook damping, despite the sensitivity of high-order PDEs to noise [17, 18]. The work presented in this paper is an extension of the work published in a recent paper [19], in which a PINN-based framework has been introduced to identify beam structures, estimating both transverse displacement and complex elastic modulus directly in the frequency domain. The contribution is based on the identification of spatially-varying elastic and damping properties in beams and plates.

Physics Informed Neural Networks (PINNs)

PINNs extend classical neural networks by embedding physical constraints into their training. A fully connected feedforward neural network with L layers and parameters $\theta = \{W^{(\ell)}, b^{(\ell)}\}_{\ell=1}^{L}$ approximates a target function $y(\mathbf{x})$ by

$$\hat{y}(\mathbf{x};\theta) = \mathcal{H}^{(L)} \circ \cdots \circ \mathcal{H}^{(1)}(\mathbf{x}), \tag{1}$$

where each layer mapping is defined as

$$\mathcal{H}^{(\ell)}(\mathbf{z}) = \sigma\Big(W^{(\ell)}\mathbf{z} + b^{(\ell)}\Big), \tag{2}$$

with σ a nonlinear activation function.

In a purely data-driven setting, training minimizes the discrete squared L^2-norm

$$\mathcal{R}_d(\theta) = \frac{1}{N}\sum_{n=1}^{N}\left|\hat{y}(\mathbf{x}_n;\theta) - y(\mathbf{x}_n)\right|^2. \tag{3}$$

Here, the set $\mathbf{x}_n$ denotes the observation points, i.e., the locations where data $y(\mathbf{x}_n)$ is available. PINNs enrich this formulation by incorporating the residual of governing PDEs. For example, consider

$$\mathcal{D}^{\alpha}(y(\mathbf{x});\lambda) = f(\mathbf{x}), \quad \mathbf{x} \in \Omega, \tag{4}$$

where $\mathcal{D}^{\alpha}$ is a differential operator parameterized by λ. This leads to the physics-informed loss

$$\mathcal{R}_f(\theta) = \frac{1}{M}\sum_{m=1}^{M}\left|\mathcal{D}^{\alpha}(\hat{y}(\mathbf{x}_m;\theta);\lambda) - f(\mathbf{x}_m)\right|^2. \tag{5}$$

where the set $\mathbf{x}_m$ denotes the collocation points, i.e., the locations in the domain where the differential equation is enforced.

The total loss $\mathcal{L}$ is then defined as a weighted combination of the two contributions:

$$\mathcal{L}(\theta) = \gamma\,\mathcal{R}_d(\theta) + \beta\,\mathcal{R}_f(\theta). \tag{6}$$

For inverse problems, unknown parameters λ can also be approximated by a neural network $\hat{\lambda}(\mathbf{x};\xi)$. This allows PINNs to jointly identify both the solution $y(\mathbf{x})$ and spatially varying properties $\lambda(\mathbf{x})$, making them particularly useful in structural dynamics for tasks such as material property mapping or damage detection.

Euler-Bernoulli Beam case

Description of the framework and its adaptation to the Euler-Bernoulli beam case

This section presents the PDE formulation of an Euler-Bernoulli model with a spatially varying elastic modulus and with a complex elastic modulus. The motion of an Euler-Bernoulli beam in permanent harmonic regime at angular frequency ω is driven by

$$\frac{\partial^2}{\partial x^2}\left(E(x)I\frac{\partial^2 w(x,\omega)}{\partial x^2}\right) - \rho S\omega^2 w(x,\omega) = f(x,\omega), \tag{7}$$

where $w = w(x, \omega)$ is the transversal deflection of the beam; I and S are the geometrical properties, corresponding to the flexural inertia $\frac{b \cdot h^3}{12}$ and the area of the cross section $h \times b$ of the beam, respectively; $E = E(x)$ and ρ [kg/m^3] are the material properties, representing the elastic modulus and density, respectively; $f = f(x, \omega)$ is the applied loading. The PDE (7) is a strong formulation, meaning the equation must be satisfied over the entire domain of the structure. This study focuses on a specific region of the beam where no external force is applied, to recover the parameters of the equation.

As the elastic modulus is non-uniform and differentiable along with the length x of the beam, and the material is linear viscoelastic, one has $E(x) = E_r(x) + jE_i(x)$, and the transversal deflection of the beam writes $w(x, \omega) = w_r(x, \omega) + jw_i(x, \omega)$. To simplify the notation, the dependence of the displacement and the complex elastic modulus on (x, ω) are omitted from now on. The loss factor η, which characterizes the material damping to be identified, is

$$\eta = \frac{E_i}{E_r}. \tag{8}$$

The problem-solving framework is presented in Figure 1. It aims at identifying the deflection of the beam and the non-constant elastic modulus, both of which are complex quantities. It includes four independent neural networks, i.e. $\hat{w}_r \approx w_r$, $\hat{w}_i \approx w_i$, $\hat{E}_r \approx E_r$ and $\hat{E}_i \approx E_i$, with parameters $\boldsymbol{\theta}_1, \boldsymbol{\theta}_2, \boldsymbol{\xi}_1$ and $\boldsymbol{\xi}_2$, respectively. For simplifying notation, $\mathcal{W} := (\hat{w}_r(\cdot; \boldsymbol{\theta}_1), \hat{w}_i(\cdot; \boldsymbol{\theta}_2))$ and $\mathcal{E} := (\hat{E}_r(\cdot; \boldsymbol{\xi}_1), \hat{E}_i(\cdot; \boldsymbol{\xi}_2))$. Therefore, the physics-informed loss function is composed of two parts [19], one related to the real terms $\mathcal{R}_f^{(\text{real})}(\mathcal{W}, \mathcal{E})$ and the other involving the imaginary terms $\mathcal{R}_f^{(\text{imag})}(\mathcal{W}, \mathcal{E})$, see Fig. 1 for the expressions.

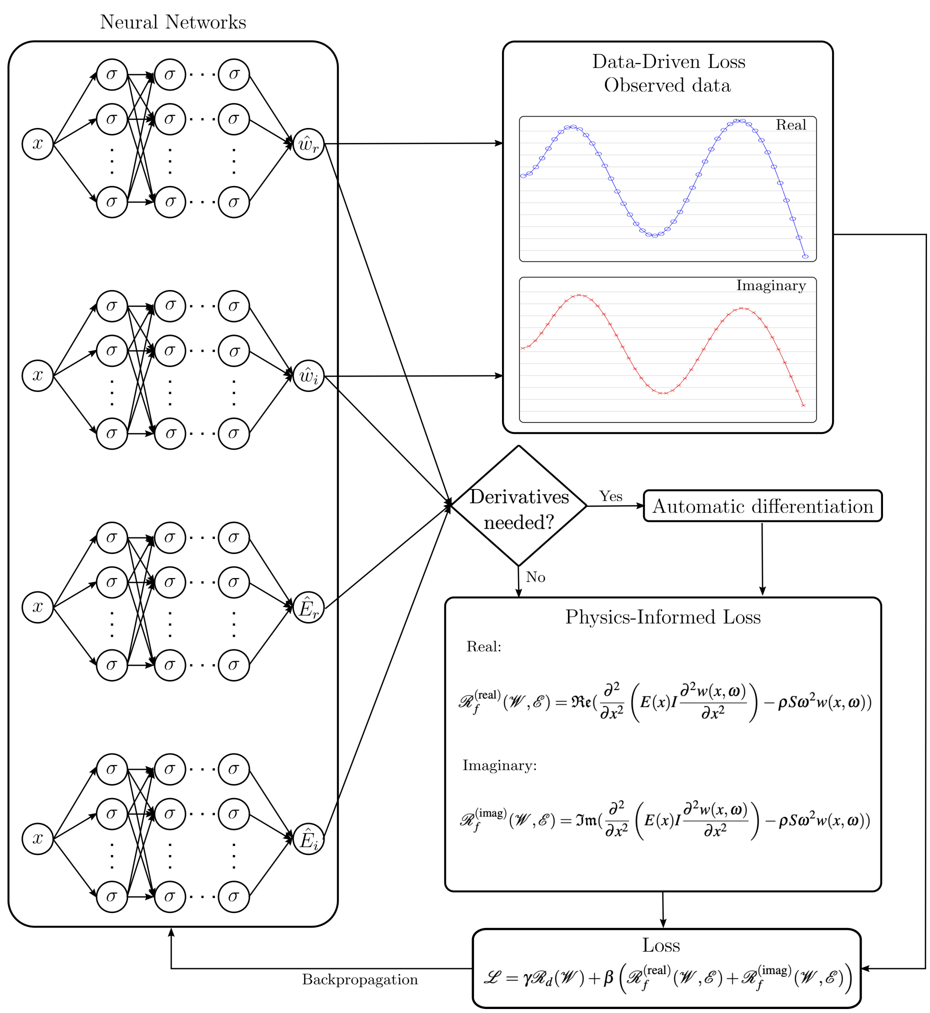

Fig. 1 PINN framework

In a similar manner, residual terms related to data observations can also be defined concerning real and imaginary components, resulting in

$$\mathcal{R}_d(\mathcal{W}) = \frac{1}{N_x}\sum_{n=1}^{N_x}\left|\hat{w}_{r,n} - w_{r,n}\right|^2 + \frac{1}{N_x}\sum_{n=1}^{N_x}\left|\hat{w}_{i,n} - w_{i,n}\right|^2, \tag{9}$$

where $\hat{w}_{\cdot,n}$ and $w_{\cdot,n}$ are the displacements evaluated at $\boldsymbol{x}_n$, and N_x corresponds to the number of points used for displacement measurements along the length of the beam. Finally, the loss function is given by

$$\mathcal{L} = \gamma\mathcal{R}_d(\mathcal{W}) + \beta\left(\mathcal{R}_f^{(\text{real})}(\mathcal{W},\mathcal{E}) + \mathcal{R}_f^{(\text{imag})}(\mathcal{W},\mathcal{E})\right), \tag{10}$$

where (γ,β) are determined heuristically. $\gamma = 1$ and $\beta = 10^{-2}$ are used in the following study.

Within the Euler Bernoulli theory, the strong form PDE involves the fourth spatial derivative of the transverse displacement. Spectrally, the operator scales like k^4, k being the wavenumber: small oscillations in the solution displacement field stemming from noise, overfitting, or numerical approximations are strongly magnified in the residual. As a consequence, residual minimization can become stiff and a naive optimizer may reduce the loss by injecting short wavelength oscillations into the inferred modulus. Our design avoids numerical differentiation of measurements, adopts smooth low variance representations for material fields, and relies on automatic differentiation for high order terms, which collectively mitigates this issue without changing the training pipeline.

Application to the identification of the properties of a beam equipped with a viscoelastic patch

Additionally to the cases already presented in [19], the efficiency of the method is tested on a case with radical properties change: a homogeneous steel beam partially covered with a viscoelastic patch. The 1-meter long cantilever beam (section 20×2 mm^2) has a loss factor of 0.5% and is excited by a point force located close to the clamp. A thin 10 cm-long viscoelastic patch is glued on the top surface of the beam, 70 cm away from the clamp. Its effect on the stiffness is negligible while it increases drastically the damping in the patch area. The RKU model [20] provides an equivalent loss factor of 0.5% in the uncovered zone suddenly growing to 50% in the viscoelastic patch area. From the knowledge of the displacement on a finite number of points along the beam, the network is expected to recover the displacement field on the zone covered by the measurements and identify the spatially varying elastic and damping properties. In the case illustrated below, the measurement zone covers half of the beam starting from 0.5 m away from the clamp, with 100 points regularly distributed on this area. These data are obtained from a finite element simulation.

This difficult case requires a huge number of iterations in the learning phase of the PINN to converge. Therefore, a variant is introduced to speed up the process, based on the assumption that the properties to identify are constant by parts on the beam, while the location of their changes remain unknown. To this end, this *a priori* information on the shape of spatial parameters is provided by introducing piecewise smooth plateaus separated by localized transitions (e.g., material patches, interfaces). Encoding this structure directly reduces the effective spatial bandwidth of admissible solutions and curbs spurious oscillations induced by high order derivatives. This is implemented using an arbitrary number of adjacent plateaus with smooth transitions build from sigmoids functions. Their strictly positive widths are enforced by parameterizing unconstrained raw gaps via softplus functions so that the intervals partition the beam length without overlap. The parameters fields $E_r(x)$ and $E_i(x)$ are realized by two single hidden layer networks whose hidden units are sigmoids positioned at the plateaus edges.

This *a priori* provides additional knowledge to the networks, while both the number of plateaus and their locations remain unknow and must be identified. To illustrate the efficiency of the method, 6 bounded plateaus with learnable edges and amplitudes are trained, while only 3 would be necessary to recover the exact solution. The results in terms of displacements are shown in Figure 2. The model preserves an accurate fit to complex displacements across the measured span, yielding smooth predictions between sensors thanks to the physical residual.

The architecture of the network is based on the one presented in [19], except the two parts related to the estimation of the mechanical properties whose networks are replaced by the plateaus-based approach described above.

The identified moduli show plateau–like behavior with physically plausible transitions. The loss modulus E_i is non negative and localized within the patch; E_r recovers steel levels outside, as illustrated in Figure 3.

This illustrates the ability of the framework to handle complex cases with radical changes in the mechanical properties, in particular the damping, whose estimation remains a challenge in structural dynamics. The methods requires the measurement of the displacement over a part of the structure, without the need to measure the input force and without the requirement to know the boundary conditions. This choice to localize informations in the training explains the behavior of the predicted modulus at the boundary of interval $[0.5, 1.0]$ in Figure 3, that is not to be taken into account. The next section aims at extending the approach to plates.

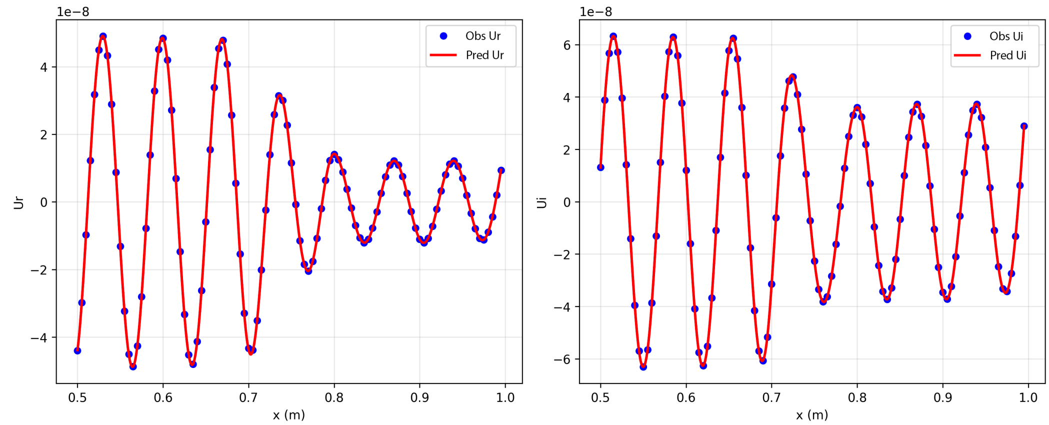

Fig. 2 Observed vs. predicted complex displacements at 4 kHz over the measured region for the 6 plateaus model

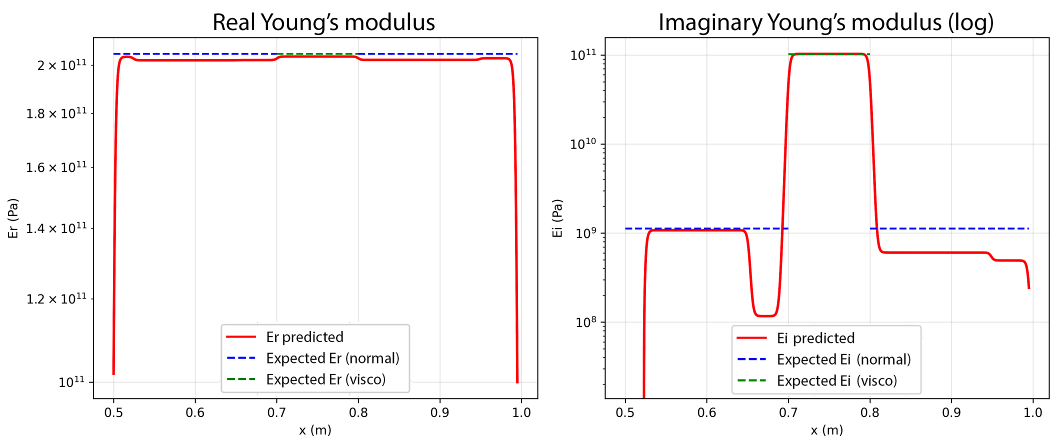

Fig. 3 Results with 6 learnable bounded plateaus: predicted real (left) and imaginary (right) parts of the modulus. Clean plateaus and physically plausible transitions are obtained.

Kirchhoff plate case

The framework introduced in [19] can be extended to any mechanical system whose movement is driven by a PDE. This section describes the basics of its application to a Kirchhoff plate, whose behaviour under harmonic motion at angular frequency ω is driven by [21]

$$-\rho h\omega^2 w + \frac{\partial^2}{\partial x^2}\left(D(x,y)\,\frac{\partial^2 w}{\partial x^2}\right) + 2\,\frac{\partial^2}{\partial x\partial y}\left(D(x,y)\,\frac{\partial^2 w}{\partial x\partial y}\right) + \frac{\partial^2}{\partial y^2}\left(D(x,y)\,\frac{\partial^2 w}{\partial y^2}\right) = q(x,y), \tag{11}$$

with ρ the density, h the thickness, $w(x,y)$ the transverse displacement, $q(x,y)$ the distributed transverse load and $D(x,y) = \frac{E(x,y)h^3}{12(1-\nu^2)}$ the bending modulus with $E(x,y)$ is the elastic modulus and ν the Poisson ratio. The split in real and imaginary parts required to define the physical losses leads to

$$-\rho h\omega^2 w_r + \partial^2_{xx}(D_r\, w_{r,xx} - D_i\, w_{i,xx}) + 2\,\partial^2_{xy}(D_r\, w_{r,xy} - D_i\, w_{i,xy}) + \partial^2_{yy}(D_r\, w_{r,yy} - D_i\, w_{i,yy}) = q_r, \tag{12}$$

$$-\rho h\omega^2 w_i + \partial^2_{xx}(D_r\, w_{i,xx} + D_i\, w_{r,xx}) + 2\,\partial^2_{xy}(D_r\, w_{i,xy} + D_i\, w_{r,xy}) + \partial^2_{yy}(D_r\, w_{i,yy} + D_i\, w_{r,yy}) = q_i, \tag{13}$$

with $\partial^2_{\alpha\beta} = \frac{\partial^2}{\partial\alpha\beta}$ and $w_{\gamma,\alpha\beta} = \frac{\partial w^2_\gamma}{\partial\alpha\beta}$.

To validate the proposed framework, a benchmark numerical experiment is first conducted using an aluminum plate (0.7 m $\times$ 0.8 m $\times$ 0.002 m) with homogeneous properties ($\eta = 0.2\%$). Four neural networks are employed: two for the displacement (one for the real part and one for the imaginary part) and two for the real and imaginary parts of the complex modulus E. All networks use an architecture with 5 hidden layers and 40 neurons per layer, with $tanh$ as the activation function. 900 collocation points are used for the evaluation of the PDE, while 64 observation points are used to feed the network with virtual measurements. A maximum learning rate of 0.001 and 0.0001 was used for the displacement and modulus networks, respectively.

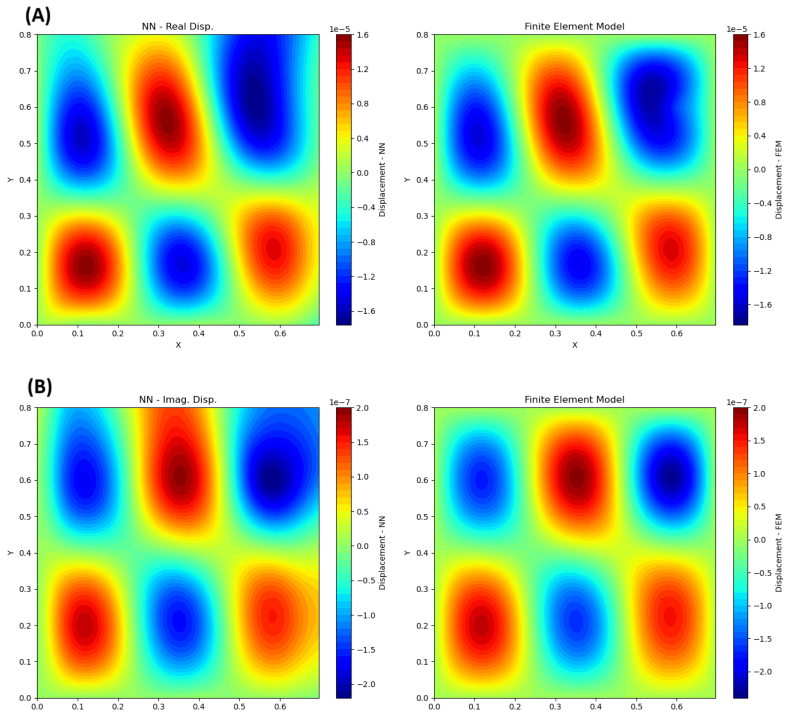

Fig. 4 Real (A) and imaginary (B) components of displacements at 130 Hz over the measured region for the homogeneous plate: PINN estimates (left) and FEM reference (right)

As illustrated in figure 4, the network provides a reasonably accurate estimation of both the real and complex components of the displacement field, even with a relatively limited number of observation points (64). The most pronounced deviations are observed near the boundary regions, which is consistent with the fact that the boundary conditions were not explicitly included in the network's prior knowledge.

The figure 5 shows the spatial distributions of the identified mechanical properties. The elastic modulus is estimated to be nearly constant over the entire surface, with variations on the order of one percent. The loss factor is predicted with good average accuracy (0.21% instead of 0.2%), although more pronounced spatial fluctuations are observed (ranging approximately from 0.1% to 0.3%). While these results are already encouraging, further improvements are expected through additional refinement of the network architecture and its hyperparameters.

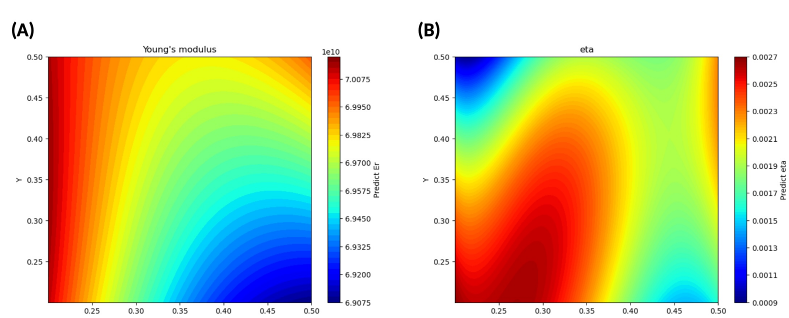

Fig. 5 Identified properties of the homogeneous plate: elastic modulus (A) and loss factor (B)

Finally, the case of a non-homogeneous conservative plate ($\eta = 0$) is investigated. A spatial variation of the elastic modulus is introduced in the vicinity of the point (0.35, 0.35), where this local reduction simulates, for instance, a defect to be identified in a structural health monitoring (SHM) framework. The displacement field at an arbitrary frequency is computed, and 64 measurement points are employed for network training.

The displacement field is shown in figure 6. Despite its spatial complexity, it is remarkably well estimated by the network. As expected, the estimation is least accurate in the vicinity of the boundary conditions.

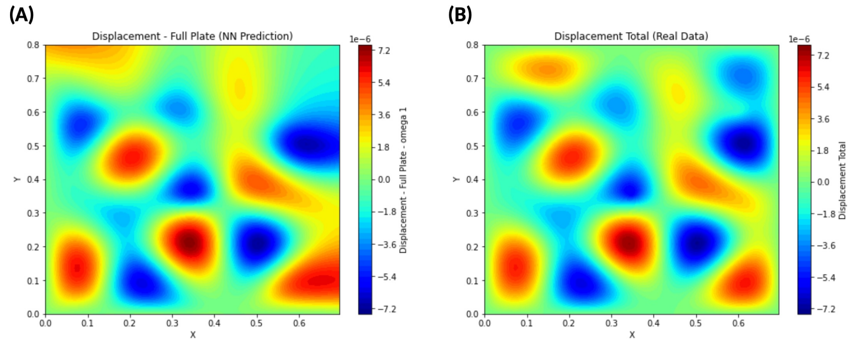

Fig. 6 Displacement at 295 Hz over the measured region for the non-homogeneous plate: PINN estimates (A) and FEM reference (B)

Figure 7 presents the elastic modulus identified by the network alongside the reference values. While the identification of the damaged region is not perfect, its location is correctly captured. These results demonstrate that the proposed approach offers promising perspectives for structural health monitoring.

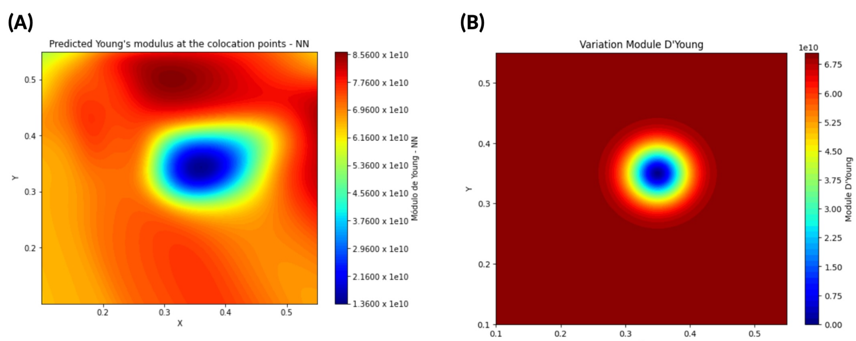

Fig. 7 Identified elastic modulus of the non-homogeneous plate (A) and reference (B)

Conclusion

The proposed method has proven effective for solving inverse problems, accurately identifying structures even without prior knowledge of boundary conditions. More specifically, the main contributions of this paper are:

- the extension of the PINN framework presented in [19] for inverse identification of a spatially rapidly-varying complex elastic modulus in an Euler-Bernoulli beam. A bounded plateaus parameterization that separates geometry from amplitude levels has been introduced. The parameter network is a shallow, single-hidden-layer sigmoid network whose units coincide with plateaus edges, while the state networks remain standard smooth multilayer perceptrons. The learnable plateaus deliver interpretable fields with plateau-like regions, localized loss, and expected levels outside the patch, all while preserving accurate displacement fits. Embedding simple geometric structure directly into the material field thus turns good fits into credible reconstructions under sparse sensing and high-order physics. Future work will investigate robustness to noise, multi-frequency excitation, experimental validation and automatic selection of the number of plateaus.
- the application of the framework introduced in [19] for the inverse analysis of thin plates. For homogeneous damped plates, the networks reliably estimate the Young's modulus and the loss factor. While exact predictions for non-

homogeneous plates remain challenging, the algorithm successfully identified damaged regions, highlighting its potential for structural health monitoring. Future work will focus on fully experimental datasets, but also to the extension of the bounded plateaus approach for 2D applications so that rapidly-varying local changes in the mechanical properties can be quantitatively computed by the machine learning tool.

Acknowledgments The authors acknowledge the support of EIPHI (ANR-17-EURE-0002).

References

1. Cross, E.J., Gibson, S.J., Jones, M.R., Pitchforth, D.J., Zhang, S., and Rogers, T.J. *Physics-Informed Machine Learning for Structural Health Monitoring*, pages 347–367. Springer International Publishing, Cham (2022)ifnextchar.gobble.
2. Aguirre, L.A. *An Introduction to Nonlinear System Identification*, pages 133–154. Springer Nature Switzerland, Cham (2024)ifnextchar.gobble.
3. Karniadakis, G.E., Kevrekidis, I.G., Lu, L., Perdikaris, P., Wang, S., and Yang, L. "Physics-informed machine learning". *Nature Reviews Physics*, 3(6):422–440 (2021)ifnextchar.gobble.
4. Raissi, M., Perdikaris, P., and Karniadakis, G. "Physics-informed neural networks: A deep learning framework for solving forward and inverse problems involving nonlinear partial differential equations". *Journal of Computational Physics*, 378:686–707 (2019)ifnextchar.gobble.
5. Henkes, A., Wessels, H., and Mahnken, R. "Physics informed neural networks for continuum micromechanics". *Computer Methods in Applied Mechanics and Engineering*, 393:114790 (2022)ifnextchar.gobble.
6. Amini Niaki, S., Haghighat, E., Campbell, T., Poursartip, A., and Vaziri, R. "Physics-informed neural network for modelling the thermochemical curing process of composite-tool systems during manufacture". *Computer Methods in Applied Mechanics and Engineering*, 384:113959 (2021)ifnextchar.gobble.
7. Mao, Z., Jagtap, A.D., and Karniadakis, G.E. "Physics-informed neural networks for high-speed flows". *Computer Methods in Applied Mechanics and Engineering*, 360:112789 (2020)ifnextchar.gobble.
8. Rezaei, S., Harandi, A., Moeineddin, A., Xu, B.X., and Reese, S. "A mixed formulation for physics-informed neural networks as a potential solver for engineering problems in heterogeneous domains: Comparison with finite element method". *Computer Methods in Applied Mechanics and Engineering*, 401:115616 (2022)ifnextchar.gobble.
9. As'ad, F. and Farhat, C. "A mechanics-informed deep learning framework for data-driven nonlinear viscoelasticity". *Computer Methods in Applied Mechanics and Engineering*, 417:116463 (2023)ifnextchar.gobble.
10. Zhai, W., Tao, D., and Bao, Y. "Parameter estimation and modeling of nonlinear dynamical systems based on Runge–Kutta physics-informed neural network". *Nonlinear Dynamics*, 111(22):21117–21130 (2023)ifnextchar.gobble.
11. Lai, Z., Mylonas, C., Nagarajaiah, S., and Chatzi, E. "Structural identification with physics-informed neural ordinary differential equations". *Journal of Sound and Vibration*, 508:116196 (2021)ifnextchar.gobble.
12. Di Lorenzo, D., Champaney, V., Marzin, J., Farhat, C., and Chinesta, F. "Physics informed and data-based augmented learning in structural health diagnosis". *Computer Methods in Applied Mechanics and Engineering*, 414:116186 (2023)ifnextchar.gobble.
13. Zhou, W. and Xu, Y. "Damage identification for plate structures using physics-informed neural networks". *Mechanical Systems and Signal Processing*, 209:111111 (2024)ifnextchar.gobble.
14. Kapoor, T., Wang, H., Núñez, A., and Dollevoet, R. "Physics-informed neural networks for solving forward and inverse problems in complex beam systems". *IEEE Transactions on Neural Networks and Learning Systems*, page 1–15 (2023)ifnextchar.gobble.
15. Faroughi, S., Darvishi, A., and Rezaei, S. "On the order of derivation in the training of physics-informed neural networks: case studies for non-uniform beam structures". *Acta Mechanica*, 234(11):5673–5695 (2023)ifnextchar.gobble.
16. Wu, W., Daneker, M., Jolley, M.A., Turner, K.T., and Lu, L. "Effective data sampling strategies and boundary condition constraints of physics-informed neural networks for identifying material properties in solid mechanics". *Applied Mathematics and Mechanics*, 44(7):1039–1068 (2023)ifnextchar.gobble.
17. Pezerat, C. and Guyader, J. "Force analysis technique: reconstruction of force distribution on plates". *Acta Acustica united with Acustica*, 86(2):322–332 (2000)ifnextchar.gobble.
18. Leclère, Q., Ablitzer, F., and Pézerat, C. "Practical implementation of the corrected force analysis technique to identify the structural parameter and load distributions". *Journal of Sound and Vibration*, 351:106–118 (2015)ifnextchar.gobble.
19. Teloli, R.d.O., Tittarelli, R., Bigot, M., Coelho, L., Ramasso, E., Le Moal, P., and Ouisse, M. "A physics-informed neural networks framework for model parameter identification of beam-like structures". *Mechanical Systems and Signal Processing*, 224:112189 (2025)ifnextchar.gobble.
20. Ungar, E.E., Ross, D., and Kerwin Jr, E.M. "Damping of flexural vibrations by alternate viscoelastic and elastic layers". Technical report (1959)ifnextchar.gobble.
21. Timoshenko, S. and Woinowsky-Krieger, S. "Theory of plates and shells" (1959)ifnextchar.gobble.